Nigerian Research Journal of Engineering and Environmental Sciences 7(1) 2022 pp. 156-167
p ISSN: 2635-3342; e ISSN: 2635-3350

Nigerian Research Journal of Engineering and Environmental Sciences
Journal homepage: www.rjees.com

Original Research Article

Artificial Neural Network for Modelling the Performance of Carbonyl-Iron Particle-Paraffin Oil-Based Magneto-Rheological Fluid

***Emagbetere, E. and Zuokumor, K.C.**

Department of Mechanical Engineering, College of Engineering and Technology, Federal University of Petroleum resources, Effurun, Nigeria.
*emagbetere.eyere@fupre.edu.ng

http://doi.org/10.5281/zenodo.6722564

ARTICLE INFORMATION

Article history:
Received 19 May, 2022
Revised 08 Jun, 2022
Accepted 10 Jun, 2022
Available online 30 Jun, 2022

Keywords:
Smart material
Magnetic particles
Grease
Rheological properties
ANN modelling

ABSTRACT

This work investigated the effectiveness of artificial neural network (ANN) for modelling the performance characteristics of a new magneto-rheological fluid (MRF). The MRF was developed from paraffin oil, carbonyl-iron particle and grease. The performance characteristics were investigated experimentally to ascertain the effects of magnetic field strength, the proportion by mass of carbonyl-iron particle and grease on the yield strength and the sedimentation ratio of the fluid. Then ANN was developed based on experimental data, and its performance was evaluated using R-square and mean square error values. The yield strength of the developed MRF was significantly affected by the percentage of carbonyl-iron particle added and the magnetic field strength. On the other hand, the proportion of carbonyl-iron particles and grease additive affected the sedimentation ratio. The developed ANN performed satisfactorily for all data sets used for training, validation and testing of the model. The error between predicted responses and those of experiments were very similar, having values of R-square close to 1. Overall, the artificial neural network was an effective tool for modelling the rheological performance of the magneto-rheological fluid.

1. INTRODUCTION

A magneto-rheological fluid (MRF) is a smart material whose rheological properties change in the presence of a magnetic field. To a high degree, MRFs remain the highest researched and applied type of smart material due to their favourable advantages (Wang et al., 2018). They are applied in different devices such as dampers, clutches, breaks, prosthetics, and polishing (Park et al., 2010; Ahamed et al., 2018). Commercially available

MRF are prepared by mixing carbonyl iron magnetic particles with silicone oil-based fluid, and some additives are added to enhance the performance (Ashtiani et al., 2015).

Due to the high cost of silicone oil, concatenated efforts have been made towards developing new types of MRF from cheap and readily available fluids (Kumar et al., 2019). Also, development of an MRF requires a degree of predictability for ease of their use in MRF devices. As new MRF types are developed, research efforts are geared towards developing suitable models that can be used for simulating MRF characteristics.

In the early years of MRF development, the focus was to identify the yield stress and viscosity affected by magnetic field and shear rate (Berli and Vicente, 2012). Noting that an MRF does not behave like a Newtonian fluid when in contact with a magnetic field, researchers adopted the Bingham model for its investigation. The Bingham model, which relates shear stress to shear rate, assumes that the fluid is viscoplastic (Wang and Gordaninejad, 20006). Later on, based on specific advantages, other viscoplastic models were adopted for modelling the rheological behavior. Some of these models include the Herschel–Buckley (Fang et al., 2009), Casson (Mitsoulis, 2007), Biviscous (Goldasz and Sapinski, 2012) and Papanastasiou (Papanastasiou, 1987). Further details of these models, as applied to MRFs, can be found in the reviews done by Ghaffari et al. (2014) and Ashtiani et al. (2015). Several studies have shown discrepancies in the results obtained using these models. It was discovered that these models offer a level of inconsistency with experimental results at low shear rates (Claracq et al., 2004). Also, some show a low level of fitting accuracy (Kim et al., 2013), and some are more suitable for specific conditions than others (Au et al., 2015). Moreover, negative values of dynamic yield stress have been obtained using some models (Rabbani et al., 2017).

Quite early enough, it was discovered that other factors, besides magnetic field and shear rate, matters when characterizing MRFs. So, several different models were developed to predict yield stress and other variables as affected by different factors. Some models estimate the yield stress from the magnetic field (Claracq et al., 2004; Piao et al., 2015). A model that captures both temperature and magnetic field to determine yield stress has been reported (Sahin et al., 2009; Guerrero-Sanchez et al., 2009; Rabbani et al., 2015). Therefore, one major problem is to seek a model that can suitably take several varying factors that may significantly affect MRF performance.

Evolutionary algorithms could address specific challenges with modelling MRF behavior. A number of artificial intelligence (AI) techniques have been applied in the modelling of MRF properties. The application of AI to modelling the magnetic behavior of some magnetic nano-particles has been reviewed by (Bahiraei et al., 2019). In their review, different AI models were used to predicted the rheological behavior using magnetic field and other varied MRF properties. AI techniques applied so far include support vector machine (Rabbani et al., 2017; Li et al., 2020), ant colony and bee combined technique (Xu et al., 2017), Fruitfly algorithm (Yu et al., 2016), artificial neural network (ANN) and deep learning (Bahiuddin et al., 2018).

The use of artificial neural network for modelling and predicting responses has some advantages, including the ability to handle multiple responses, nonlinearity, and noise with good speed and high accuracy (Lee and Chen, 1993; Bahiraei et al., 2019). A particular report presented the modelling of magneto-rheological materials with ANN, which has aided the easy predictability of viscosity and thermal conductivity of Ferrite, silicone oil-based MRF (Esfe et al., 2017). Another work discussed yield stress prediction based on magnetic field and concentration of particles for water-based magnetite ferrofluid using ANN (Shahsavar et al., 2020). Rabbani et al. (2017) developed an ANN that can effectively be used to predict the dynamic yield stress from temperature, field strength and shear rate for carbonyl iron particle (CIP) based MRF. Razi et al. (2014) applied ANN to model the rheological behavior of MRF prepared using CIP and Xantham gum as additives. The findings of existing research that applied ANN for modelling of rheological properties of MRF cannot be satisfactorily used to make a general conclusion on the effectiveness of ANN for modelling MRFs, particularly the emerging types. More so, the effectiveness of ANN for modelling several other influencing factors and outputs variables of MRF is yet to be investigated.

Therefore, this work aims to investigate ANN's effectiveness in modelling and predicting the performance characteristics of a CIP and paraffin oil-based magneto-rheological fluid that is enhanced with grease. Specific objectives to be pursued includes to develop the MRF following standard procedure, obtain the performance characteristics for different samples, developed an ANN model, and investigate the performance of the model for predicting its performance characteristics.

2. MATERIALS AND METHODS

2.1. Materials

This research made use of magnetic particles (Carbonyl Iron particle of size range 3-5 um, obtained via Aliexpress from Chengdu Huarui Industrial Co. Ltd, China), carrier fluid (Paraffin oil of viscosity of 32 mPa, density of 0.8 g/cm3 at room temperature, obtained from O and J Chemical Store, Delta State, Nigeria), additive (Lithium grease, type: Filtex, obtained locally). Other items include water and petrol.

2.2. Samples Preparation

Sixteen samples were prepared following the standard procedure (Ashanti et al., 2015; Guo et al., 2018), which involved measuring the proportion of each constituent needed, mixing appropriately and using as needed. The mixing proportion of CIP and added additive for the 16 samples were based on a 3 level, Taguchi experimental design, and the upper and lower limits are shown in Table1. The selected values were similar to range of values reported in the literature (Chin et al., 2001; Gopinath et al., 2020). The weight of CIP, paraffin oil and lithium grease needed to prepare the desired sample were measured using a beam balance. The measured CIP was mixed with the measured grease and stirred for 10 minutes at 2000 rpm using a mechanical stirrer, and poured into a beaker containing the paraffin oil. They were then stirred further at 2000 rpm using the mechanical stirrer for five (5) minutes. After stirring sufficiently, the samples were used for experiments.

Table 1: Upper and lower limits of variables for experimental samples

Factors	Name of variable	Lower bound	Upper bound
A	Weight of CIP (wt%)	40	70
B	Weight of Additives (wt%)	0	3
C	Magnetic field strength (T)	0.5	1.5

2.3. Experiments

The goal of the experiments was to obtain valuable data needed for building and testing the ANN. The viscosity for the different samples was measured with a viscometer. The magnetic field was induced to the sample using a locally developed magnetic device shown in Figure 1. Each sample was tested for a magnetic field strength of 0.5, 1.0, 1.2 and 1.5 T, based on the capability of the magnetic device. Thus, a total of 64 tests carried out in all.

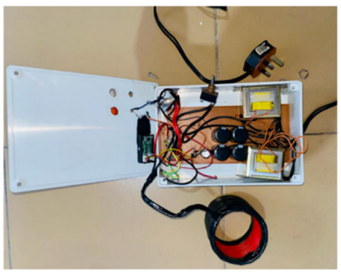

Figure 1: Electromagnetic device used to induce magnetic field into the developed MRF

Experimental data of shear stress as affected by shear strain were obtained with the aid of a rheometer. Different portions of the developed samples were then assessed for rheological responses: viscosity and shear stress, for varied magnetic fields and shearing speeds. After that, the yield stress, a major characteristic parameter for MRF, was determined using the Bingham model (Equation 1), which is the most utilised and simplified form of rheological models (Ghaffari et. al., 2014). τ is the shear stress, τ_y is the yield stress, μ is the viscosity and $\dot{\gamma}$ is the shear rate.

$$\tau = \tau_y + \mu\dot{\gamma} \tag{1}$$

The visual inspection or direct method was applied to determine the stability of the developed MRF. The method is widely applied to investigate the stability of MRF (Guo et al., 2018). Here, visual inspection was used to estimate the rate at which the iron particles settled in each of the MRF samples. This was achieved by comparing the heights of the suspended particles and the total height of the prepared sample after leaving for 24 hrs. The height of the suspended phase (H_{sp}) and the settled phase (H_{st}) were obtained using a calibrated beaker containing the MRF sample. Equation 2 was used to estimate the sedimentation ratio (R_{sd}) for each sample.

$$R_{sd} = \frac{H_{sp}}{H_{sp}+H_{st}} \tag{2}$$

2.4. Development of Artificial Neural Network Model

The artificial neural network developed was based on the experimental data described in section 2.3. The sole aim was to build an ANN-based MRF model useful for both predictions and simulation purposes. The fitting tool of the neural network graphics user interface (GUI) in MATLAB was used for developing the ANN. It was a feed-forward multi-layer network which was built with three inputs consisting of magnetic field strength, percentage mass of CIP and the additive, while yield stress and sedimentation ratio served as outputs. A total of 64 entries from the experiment were used to train the network. Varied number of hidden neurons 10, 12 and 20 were employed in setting the network on different occasions to ascertain the best number of hidden neurons for optimum performance of the network. The data was split into three sets, and 70% (44) was used to train the network, 15% (10) was used for validation of the network, and 15% (10) was used to test the network after training. The network was trained using the Levenberg-Marquardt algorithm by adjusting the weights associated with the neurons based on Equation 3. The network's performance was evaluated using the mean square error and comparing R-values of the generated regression plots and error histograms.

$$A_i = f\sum_{i=1}^{N_i}[Bm + C]_i \tag{3}$$

Where f is the operating function, Ni is the ith input, B is the connection weights, C is the bias, m is the ith input and Ai is ith output of an ANN.

2.5. Analysis of Variance

The variance within and between the experimental data set and the predicted values using the developed ANN was estimated using the ANOVA solver in Microsoft Excel version 2013. The P-values were calculated at a 5 % confidence level, and it helped ascertain if there were significant variation in the data set.

2.6. Performance Assessment of the ANN Model

The errors were estimated for both data obtained from experiments and those predicted using the developed ANN. Two statistical metrics were used, and they were the correlation coefficient (R) shown in Equation (4) and the coefficient of determination (R^2) shown in Equation 5. The residual standard error measures the

absolute difference between predicted and experimental values. In contrast, R-square values provides information on the percentage of the variance of the dependent variable explained by the ANN. Then also, the mean square error (MSE) shown in Equation 6 was used to estimate the mean value of error between the experimental and predicted values.

$$R = \left(\frac{\sum_{i=1}^{n}(Y_{p.i}-\bar{Y}_p)(Y_{ex.i}-\bar{Y}_{ex})}{\sqrt{\sum_{i=1}^{n}(Y_{p.i}-\bar{Y}_p)^2 \sum_{i=1}^{n}(Y_{ex.i}-\bar{Y}_{ex})^2}}\right) \quad (4)$$

$$R^2 = 1 - \frac{\sum_{i=1}^{n}(Y_{p.i}-Y_{ex.i})\text{^}2}{\sum_{i=1}^{n}(Y_{p.i}-\bar{Y}_{ex})^2} \quad (5)$$

$$MSE = \frac{1}{n}\sum_{i=1}^{n}(Y_{ex.i} - Y_{p.i})^2 \quad (6)$$

n is the total number of samples, i is the sample/serial number, $Y_{p.i}$ is the ith predicted outcome, $\bar{Y}_p$is the average value of predicted outcomes, $Y_{ex.i}$ is the ith experimental value, and $\bar{Y}_{ex}$ is the average of the experimental values.

3. RESULTS AND DISCUSSION

3.1. Characteristics of the Developed MRF

The effect of the constituting amount of CIP and additive (grease) on the yield stress is shown in Figure 2. As evident, the yield stress rose uniformly as the mass of CIP increased, and the ratio of yield stress and mass of CIP was constant for all values of additives added. Yield stress is known to increase with the addition of magnetic particles, as reported in the literature (Gopinath et al., 2020). However, increasing the proportion of magnetic particles negatively affects the dispersion stability. Hence additives are usually applied. For this study, the addition of additive (grease) does not affect the values of yield stress significantly (P>0.05). So generally, the addition of grease up to 9.228 g (3 %) does not show any significant effect on the yield stress for CIP-paraffin oil-based MRF.

The sedimentation ratio was determined using Equation 3, and the values for different samples as affected by the mass of CIP and grease that was added is shown in Figure 3. It can be observed that the value of the sedimentation ratio increased as the mass of grease increased from 0 to 9.228 g. Additionally, for a particular mass of grease, increasing the proportion of CIP resulted in decreasing sedimentation ratio. The sedimentation is the major challenge facing MRF (Kumar et al., 2019), and grease has been reportedly used to tackle sedimentation of some other MRF types (Chin et al., 2001; Kumar et al., 2019). In like manner, the application of grease is shown to have reduced the sedimentation for CIP-paraffin based MRF in this study.

Figure 4 gives the relationship between yield stress and CIP for varied field strength. It can be seen that for all masses of CIP employed in the experiment, the yield stress increased uniformly with increasing in field strength varied from 0.5T – 1.5T. The dependency of the yield strength on the magnetic field confirms its capability to serve as a suitable MRF material. This is a description of the intelligent behaviour of the CIP-paraffin oil-based MRF. MRFs are widely adopted based on the ability of their rheological property to change in the presence of a magnetic field (Park, et al., 2010). Like other MRF types, yield strength is known to increase with magnetic field due to the formation of a chain-like structure of the magnetic particles (Swaroop et al., 2020).

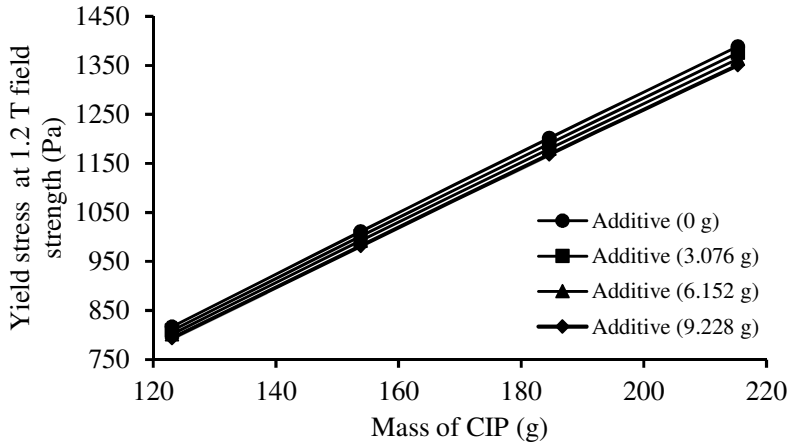

Figure 2: Graph of yield stress at 1.2 T vs mass of CIP for a varied proportion of grease

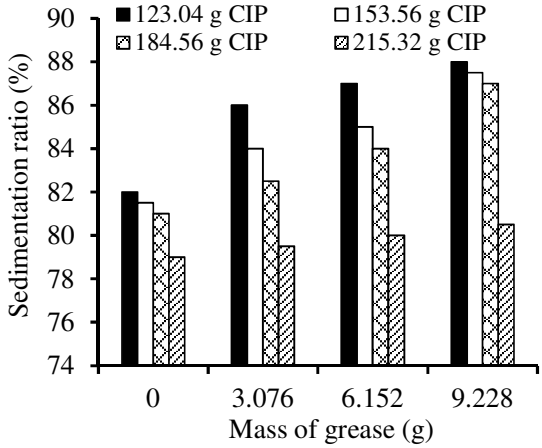

Figure 3: Graph of sedimentation ratio vs mass of grease for different masses of CIP

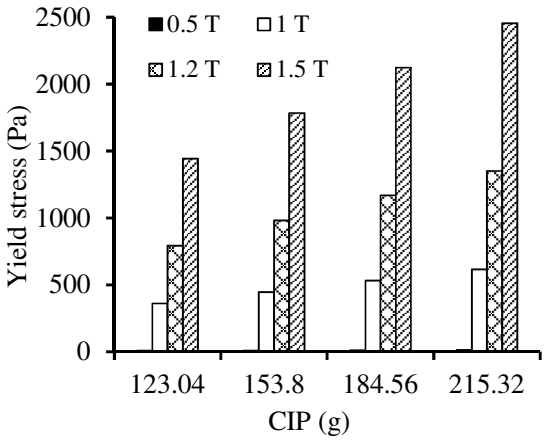

Figure 4: Graph of yield stress vs mass of CIP for different field strength

3.2. Correlation Analysis

Table 2 gives the Pearson correlation coefficient between the input variables (magnetic field intensity, proportion of additive and grease added) and the outputs (sedimentation ratio and yield strength). It is evident that the magnetic field is strongly correlated with the yield stress since the correlation coefficient is 0.92 (close to 1), but it has no correlation with sedimentation ratio, having values of correlation coefficient equal to 0. This implies that as magnetic field values go up, the yield stress would increase positively, without affecting the rate at which sediments would be form during usage. The additive does not correlate with the yield stress of the MRF (having a correlation value of -0.01, which is very close to 0, but it is positively correlated with the sedimentation ratio. This is an implication that increasing the values of additive would not significantly affect the yield stress but would improve the stability property of the CIP and parrafin oil MRF. The amount of added CIP is slightly correlated with the yield stress of the MRF, so an increase in the proportion of CIP would mean higher values of yield stress. However, proportion of CIP has a high negative correlation with sedimentation ratio, such that as the quantity of CIP in the MRF is increased for more yield strength, more particles are likely to settle with time. However, this negative effect of mass of CIP on the MRF sedimentation property can be addressed using suitable amount of additive.

Table 2: Correlation between the inputs and outputs

	Yield stress (Pa)	Sedimentation ratio (%)
Magnetic field intensity	0.92	0.00
Mass of additive	-0.01	0.59
Mass of CIP	0.23	-0.71

3.3. Performance of the Developed Artificial Neural Network

A 2 layer neural network with three inputs, ten hidden and two output neurons was found satisfactory. A number of retraining for the network helped to change the initial weights and biases of the network. The training was completed after 26 epochs. The GUI of the built artificial neural network is seen in Figure 5. Based on the error analysis discussed in the following section, the neural network performed satisfactorily after a chain of retraining and changing the numbers of hidden neurons.

Figure 6 is a performance plot of the network. It represents a highlight of the training, validation and testing errors as the number of iterations increases until there is convergence. The red, blue and green lines represent the outcome of the testing, training and validation data set, respectively. The result is reasonable as the test and validation errors have similar characteristics. Out of 30 iterations, no significant overfitting had occurred by 24 iterations. This is the point where the best validation performance occurs. The other 6 epochs showed no reasonable change in error. Thus, the network with the described specifications was considered good.

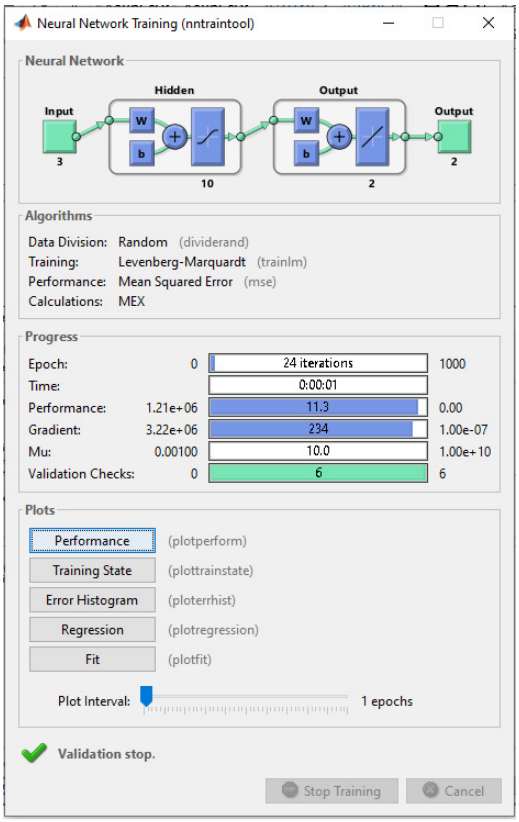

Figure 5: A screenshot of the neural network graphics showing the trained network ready for performance evaluation

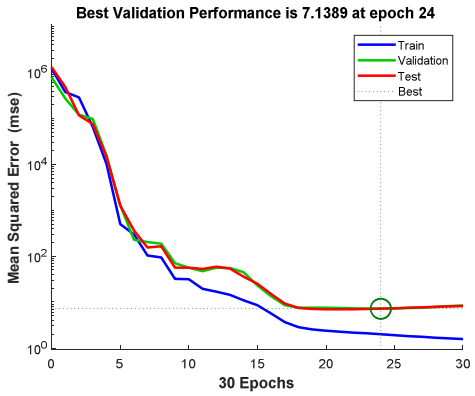

Figure 6: Performance plots of the developed neural network

The regression plots for the neural network's training, validation, and testing data sets is shown in **Error! Reference source not found.**7. It represents the network's outputs with their corresponding targets plotted on the x and y- axis, respectively. Most data sets fall along the 45-degree line where network outputs are equal to targets. The fit is reasonably good for all the data sets, with R-values being 1, 0.99999 and 0.99999 for training, validation, and testing, respectively. The R-values being very close to 1 indicates that the network properly models the input to the output. Figure 8 is the error histogram of the developed neural network. The blue, green and red bars are for the training, validation and testing dataset, respectively. This histogram shows outliers (data points where the fit is significantly worse than a majority of the data). As observed, the mean square error is -254. This result is acceptable as the final mean square error value is minimal compared to values of several other iterations.

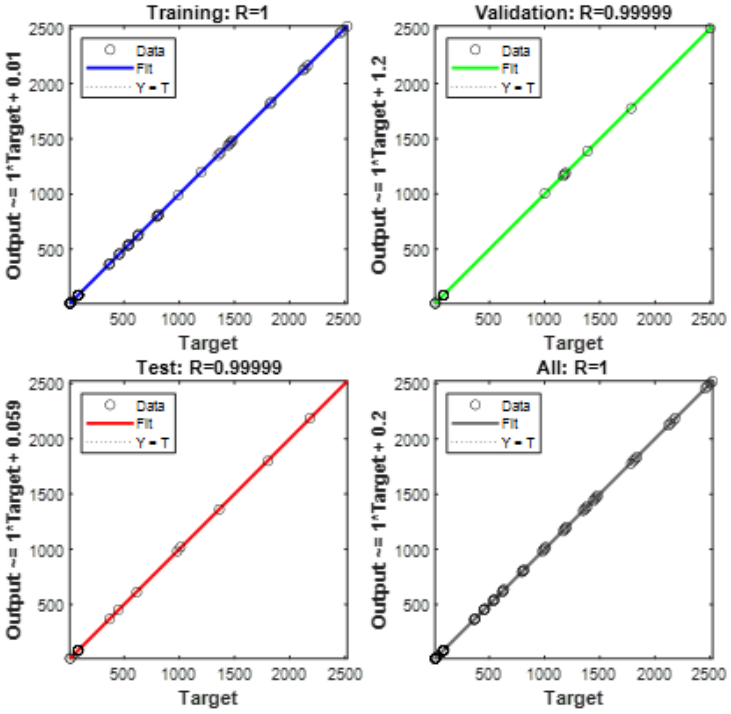

Figure 7: Regression plots for the developed neural network

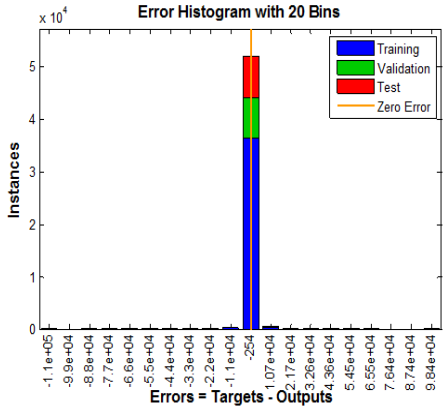

Figure 8: Error histogram for the developed network

3.4. Responses from Experiments and ANN Predicted Values

The responses from experiments and those predicted using the developed ANN were collated and presented as follows. The connection between sedimentation ratio and mass of grease added for experimental and ANN predicted values is shown in Figure 9. Analysis of variance for both values showed no significant difference with a p-value >0.05 for both cases (ANN predicted and experimental values). The sedimentation ratio was found to be higher for lower values of CIP and higher values of added grease. So the experimental data bore a similitude to the ANN data.

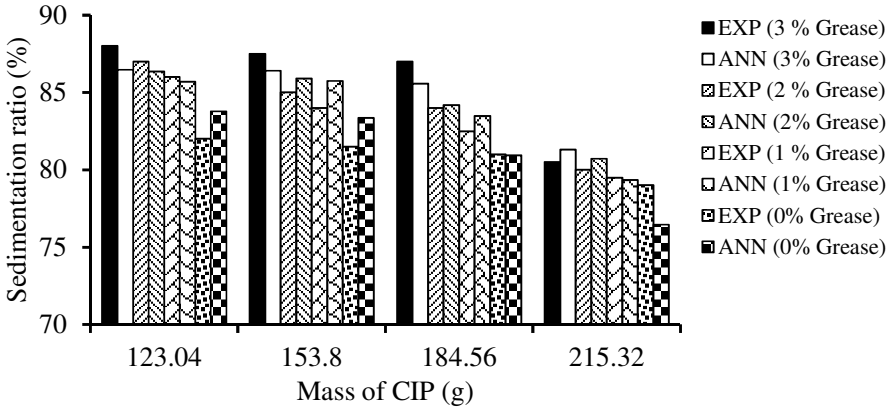

Figure 9: A graph of sedimentation ratio vs mass of grease

Figure 10 presents the result for the impact of CIP (using chosen field strength and a particular mass of additive for both experimental and ANN data) on the yield stress. As seen, yield stress took an upward stroke uniformly with an increase in mass of CIP, and for the selected mass of CIP, there was a sharp jump in yield stress as the field strength increased with no significance difference in the experimental and ANN data sets. The rate at which the yield stress increases in a magnetic field is higher than that at which it increases when there is no field strength. The values of experiments and those obtained via ANN prediction are closely related, and they do not show any significant variation statistically (having p-value greater than 0.05).

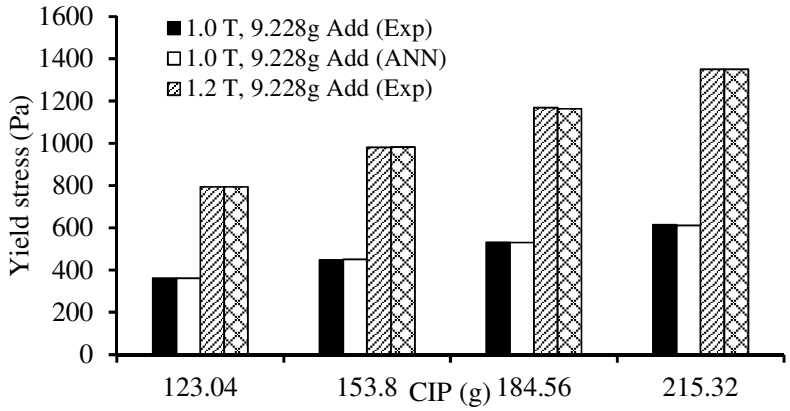

Figure 10: Graph of Yield Stress vs mass of CIP

3.5. Goodness of Fit Statistics

The extent to which the ANN predicted values correlates with those of experiments were determined using Equations 4 and 5, and the result is shown in Table 3.

Table 3: Goodness of fit

Metric	Yield stress	Sedimentation ratio
R	0.999998	0.999851624
R^2	0.999996	0.999699942
MSE	2.33587	1.316384697

It can be seen that the R and R-square values for both yield stress and sedimentation ratio are very close to 1. This implies that the ANN predicted values and experimental values are closely related. Also, the mean square error calculated based on Equation 6 is small, indicating that the ANN performs satisfactorily predicting the rheological properties of the developed MRF. The values of R and R-squared were very close to 1, indicating the near-perfect level of accuracy with which the ANN could predict outcomes. This high level of accuracy is well known for the application of ANN to the modelling and predicting multiple outputs (Bahiraei et al., 2019).

4. CONCLUSION

This work reports the effectiveness of ANN for modelling and simulating the performance of an emerging MRF type produced with CIP, paraffin oil and grease. Rheological and stability properties of the MRF were first studied. It was shown that the yield stress increase with increasing proportion of CIP and introduction of a magnetic field, but it is not affected by the addition of grease as additive. The addition of grease effectively enhanced the sedimentation property of the MRF. ANN that is made up of three inputs and two output variables performs satisfactorily when used to model the rheological and stability characteristics of the MRF. The inputs were mass of CIP, mass of grease and magnetic field strength, while the outputs were yield strength and sedimentation ratio. The positive extrapolating ability of the ANN for the novel MRF as judged by the MSE values was confirmed, and its optimal level of accuracy was also remarkably demonstrated. The correlation between variables did not affect the developed ANN, as its efficiency was high even though there was no correlation between some of the input variables and the outputs. After extrapolating outputs using the developed ANN, the errors were analyzed using several correlation coefficients. Overall, the MRF produced from CIP and paraffin oil, enhanced with grease, performs

satisfactorily, and ANN models can be adopted for the simulation of useful responses needed for its application.

5. ACKNOWLEDGMENT

The authors wish to acknowledge the assistance and contributions of the laboratory staff of Department of Petroleum and Gas Engineering and the Department of Chemical Engineering, Federal University of Petroleum Resources, Effurun, Nigeria, for their support toward the success of this work.

6. CONFLICT OF INTEREST

There is no conflict of interest associated with this work.

REFERENCES

Ahamed, R., Choi, S.-B. and Ferdaus, M. M. (2018). A state of art on magneto-rheological materials and their potential applications. *Intelligent material systems and structures,* 29(10), pp. 1-45.

Ashtiani, M., Hashemabadi, S. H. and Ghaffari, A. (2015). A review on the magnetorheological fluid preparation and stabilization. *Journal of Magnietic Material,* 374, pp. 716-730.

Au, P. I., Foo, B., Leong, Y.-K., Zhang, W. L. and Choi, H. J. (2015). Rheological analysis of graphene oxide coated anisotropic PMMA microsphere based electrorheological fluid from Couette flow geometry. *Journal of Industrial and Engineering Chemistry,* 7(5), pp. 589-593.

Bahiraei, M., Heshmatian, S. and Moayedi, H. (2019). Artificial intelligence in the field of nanofluids: A review on applications and potential future directions. *Powder Technology,* 353, pp. 276–301.

Bastola, A. K. and Hossain, M. (2020). A review on magneto-mechanical characterizations of magnetorheological elastomers. *Composites Part B,* 200, p. 108348

Berli, C. L. A. and Vicente, J. d. (2012). A structural Viscosity Model for Magnetorheology. *Applied Physics letter,* 101(021903), pp. 1-4.

Chin, B. D., Park, J. H., Kwon, M. H. and Park, O. O. (2001). Rheological properties and dispersion stability of magnetorheological (MR) suspensions. *Rheol Acta,* 40, pp. 211-219.

Claracq, J., Sarrazin, J. and Montfort, J. P., 2004. Viscoelastic properties of magnetorheological fluids. *Rheologica Acta,* 43(1), pp. 38-49.

Esfe, M. H., Bahiraei, M., Hajmohammad, M. H. and M. Afrand (2017). Rheological characteristics of MgO/oil nanolubricants: experimental study and neural network modeling. *International Communinications in Heat and Mass Transfer,* 86, pp. 245-252.

Fang, F. F., Choi, H. J. and M. S. Jhon (2009). Magnetorheology of soft magnetic carbonyl iron suspension with single-walled carbon nanotube additive and its yield stress scaling function. *Colloids and Surfaces A: Physicochemical and Engineering Aspects,* 351(1-3), pp. 46-51.

Ghaffari, A., Hashemabadi, S. H. and Ashtiani, M. (2014). A review on the simulation and modeling of magnetorheological fluids. *Journal of Intelligent Material Systems and Structures,* 26(8), pp. 1-14.

Goldasz, J. and Sapinski, B. (2012). Nondimensional characterization of flow-mode magnetorheological/electrorheological fluid dampers. *Journal of Intelligent Material Systems and Strustcures,* 23(14), pp. 1545-1562.

Gopinath, B. Sathishkumar, G., Karthik, P., Charles, M. M., Ashok, K., Ibrahim, M., & Akheel, M. M. (2020). *A systematic study of the impact of additives on structural and mechanical properties of Magnetorheological fluid*, 59, pp. 1-8

Guerrero-Sanchez, C., Ortiz-Alvarado, A. and Schubert, U. S. (2009). Temperature effect on the magnetorheological behavior of magnetite particles dispersed in an ionic liquid. *Journal of Physics: Conference Series,* 149(1), p. 012052.

Guo, Y.-Q., Sun, C.-L., Xu, Z.-D. and Jing, X. (2018). Preparation and Tests of MR Fluids With CI Particles Coated With MWNTs. *Froniers in materials,* 5, pp. 1-8

Kim, Y. J., Liu, Y.D., Seo, Y. and Choi, H. J (2013). Pickering-Emulsion-Polymerized Polystyrene/Fe2O3 Composite Particles and Their Magnetoresponsive Characteristics. *Langmuir,* 29(16), pp. 4959-4965.

Kumar, J. S., Paul, P. S., Raghunathan, G. and Alex, D. G. (2019). A review of challenges and solutions in the preparation and use of magnetorheological fluids. *International Journal of Mechanical and Materials Engineering,* 14(13), pp. 1-18.

Lee, M. J. and Chen, J. T. (1993). Fluid property predictions with the aid of neural networks. *Industrial and Engineering Chemistry Research,* 32(5), pp. 995-997.

Li, S., Tian, T., Wang, H., Li Y., Li J., Zhou Y. and Wu J. (2020). Development of a four-parameter phenomenological model for the nonlinear viscoelastic behaviour of magnetorheological gels. *Materials and Design,* 194, p. 108935.

Mitsoulis, E., (2007). Flows of viscoplastic materials: models and computations. *Rheology Reviews,* 2007, pp. 135-178.

Papanastasiou, T. C. (1987). Flows of Materials with Yield. *Journal of Rheology,* 31(5), pp. 385-405.

Park, B. J., Fang, F. F. and Choi, H. J. (2010). Magnetorheology: materials and application. *Soft material,* 6, pp. 5246-5253.

Piao, S. H. Bhaumik, M., Maity, A., and Choi, H.J. (2015). Polyaniline/Fe composite nanofiber added softmagnetic carbonyl iron microsphere suspension and its magnetorheology. *Journal of Materials Chemistry C,* 3(8), pp. 1861-1868.

Rabbani, Y., Ashtiani, M. and Hashemabadi, S. H. (2015). An Experimental Study on the Effects of Temperature and Magnetic Field Strength on the Magnetorheological Fluid Stability and MR Effect. *Soft Matter,* 11, pp. 4453-4460.

Rabbani, Y., Shirvani, M., Hashemabadi, S. and Keshavarz, M. (2017). Application of Artificial Neural Networks and Support Vector Regression Modeling in Prediction of Magnetorheological Fluid Rheometery. *Colloids and Surfaces A: Physicochem. Eng. Aspects,* 520, pp. 268–278

Razi, M. M., Kelessidis, V., Maglione, R., Ghiass, M., Ghayyem, M., Razi, M. and Al., E. (2014). Experimental study and numerical modeling of rheological and flow behavior of xanthan gum solutions using artificial neural network. *Journal of Dispersion Science and Technology,* 35, pp. 1793-1800.

Sahin, H., Wang, X. and Gordaninejad, F. (2009). Temperature Dependence of Magneto-rheological Materials. *Journal of Intelligent Material Systems and Structures,* 20(18), pp. 2215-2222.

Shahsavar, A. Khanmohammadi, S., Afrand, M., Goldanlou, A. S. and Rosatami, S. (2020). On evaluation of magnetic field effect on the formation of nanoparticles clusters inside aqueousmagnetite nanofluid: An experimental study and comprehensive modeling. *Journal of Molecular Liquids,* 312, p. 113378

Swaroop, K. V., Aruna, M. N., Kumar, H. and Rahman, M. R. (2020). Investigation of steady state rheological properties and sedimentation of coated and pure carbonyl iron particles based magneto-rheological fluid. *Materials Today: Proceedings.* 39 (11), pp. 1-9

Wang, G. Ma, Y., Cui, G., Lib, N., and Dong, X. (2018). Two-dimensional Fe3O4/MoS2 nanocomposites for a magnetorheological fluid with enhanced sedimentation stability. *Soft Matter,* 4, pp. 1917--1924.

Wang, X. and Gordaninejad, F. (2006). Study of magnetorheological fluids at at high shear rates. *Rheol Acta,* 45, pp. 899-908.

Xu, Q. Chen, C., Liu, X, Li, J. and Yuan C. (2017). An ABC-BP-ANN algorithm for semiactive control for Magnetorheological damper. *KSCE Journal of Civil Engineering,* 21, pp. 2310-2321.

Yu, Y., Li, Y., Li, J. and Gu, X. (2016). Self-adaptive step fruit fly algorithm optimizeds upport vector regression model for dynamic response prediction of magnetorheological elastomer base isolator. *Neurocomputing,* 211, pp. 41-52.